Deconvolution of Images and Spectra

Second Edition

Edited by

Peter A. Jansson

E. I. DU PONT DE NEMOURS AND COMPANY (INC.)
EXPERIMENTAL STATION
WILMINGTON, DELAWARE

ACADEMIC PRESS

San Diego London Boston
New York Sydney Tokyo Toronto

To my father,
the late **John H. Jansson,**
remembered for devotion to his family,
and to the** advancment **of science and education

Couer image: See Chapter 7, Figure 14 (page 253). Used with permission.

ACADEMIC PRESS, INC.
525 B Street, Suite 1900, San Diego, CA 92101-4495, USA
1300 Boylston Street, Chestnut Hill, MA 02167, USA
http://www.apnet.com

ACADEMIC PRESS, LIMITED
24-28 Oval Road, London NW1 7DX
http://www.hbuk.co.uk/ap/

Library of Congress Cataloging-in-Publication Data

Deconvolution of images and spectra/ edited by Peter A. Jansson.-2nd ed.
p. cm.
Rev. ed. of: Deconvolution. 1984.
Includes bibliographical references and index.
ISBN o-12-380222-9 (alk. paper)
1. Spectrum analysis-Deconvolution. I. Jansson, Peter A. II. Deconvolution.
QC451.6.D45 1997
621.36' l-dc20
96-27097
CIP

Printed in the United States of America
96 97 98 99 00 EB 9 8 7 6 5 4 3 2 1

Chapter 14 Alternating Projections onto Convex Sets

Robert J. Marks II

Department of Electrical Engineering,
The University of Washington
Seattle, Washington

List of Symbols

$A, B, C, D, A_1, A_2, A_3$	sets of vectors or functions
E	the universal set
$\vec{u}_1, \vec{u}_2, \vec{v}, \vec{z}$	multidimensional vectors
$\vec{u}_A, \vec{u}_B$	vectors in the sets A and B
$u(x), v(x), u_1(x), u_2(x), w(x), z(x)$	functions of a continuous variable
$m(x)$	the middle of a signal
$U(\omega), V(\omega)$	the Fourier transforms of $u(x)$ and $v(x)$
POS	positive
BE	bounded energy
BS	bounded signals

DECONVOLUTION OF IMAGES AND SPECTRA
SECOND EDITION

ISBN: O-12-380222-9

CA	constant area
CP	constant phase
LV	linear variety
P	a projection matrix
P_S	projection onto a set S
$\mathbf{P}_m$	projection onto set m
PI	pseudo-inverse
IM	signals with identical middles
M	number of sets
$\mathscr{O}$	an operator
S	a degradation matrix
T	matrix transposition (used as a superscript)
TL	time limited
Ω	bandwidth
X	duration limit
$d(x)$	a displacement function used to define linear varieties
α	(a) $0 \leq \alpha \leq 1$ parameterizes the line connecting two vectors; (b) $\alpha > 0$ is used to define a cone in a Hilbert space
λ	relaxation parameter
β, γ	finite real numbers used to define a subspace
(x, y)	coordinates on a two-dimensional plane
$\vec{i}, \vec{o}$	image and object vectors
$\vec{o}^{(n)}$	the result of iteration n on the restoration of a discrete object
$o^{(k)}[n]$	the result of iteration k on restoration of an object, $o[n]$
$o(x)$	an object that is a function of a continuous variable
$o^{(N)}(x)$	the result of iteration N on restoration of an object of a cone
$\mathscr{H}$	a Hilbert space
$\mathscr{I}$	the imaginary part of
$\mathscr{S}$	a subspace (or linear manifold) in a Hilbert space
$\mathscr{P}$	a projection operator
$\mathscr{R}$	the real part of
$\perp \mathscr{S}$	the subspace that is the orthogonal complement of $\mathscr{S}$
$\mathscr{P}_{\mathscr{A}}$	projection operator onto a set A,
$u_{\mathscr{S}}(x)$	a function in a subspace $\mathscr{S}$
L_2	a Hilbert space with continuous variables
l_2	a Hilbert space with discrete variables
$u[n]$	element n in a sequence u

$\mathbf{1}$	an identity operator
$\{\ \}$	set
	in set notation, read "such that"
	intersection
$\in$	is an element of
$\|\cdot\|$	l_2 or L_2 norm
	perpendicular
P	the area of a signal

I. Introduction

Alternating projections onto convex sets (POCS)* [1] is a powerful tool for signal and image restoration and synthesis. The desirable properties of a reconstructed signal may be defined by several convex signal sets, which may be further defined by a convex set of constraint parameters. Iteratively projecting onto these convex constraint sets may result in a signal that contains all desired properties. Convex signal sets are frequently encountered in practice and include the sets of band-limited signals, duration-limited signals, signals that are the same (e.g., zero) on some given interval, bounded signals, signals of a given area, and complex signals with a specified phase.

POCS was initially introduced by Bregman [2] and Gubin *et al.* [3] and was later popularized by Youla and Webb [4] and Sezan and Stark [5]. POCS has been applied to such topics as sampling theory [6], signal recovery [7], deconvolution and extrapolation [8], artificial neural networks [9, 10, 11, 12, 131, tomography [1, 14, 15], and time-frequency analysis [16,17]. A superb overview of POCS with other applications is in the book by Stark [1] and the monograph by Combette [18].

II. Geometrical POCS

Although signal processing applications of POCS use sets of signals, POCS is best visualized viewing the operations on sets of points. In this section, POCS is introduced geometrically.

*The ***alternating*** term is implicit in the POCS paradigm, but traditionally is not included in the acronym.

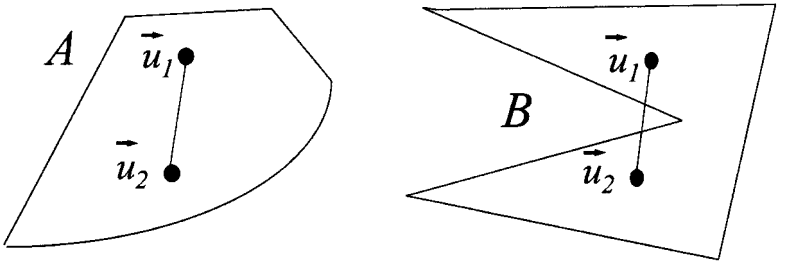

Figure 1 The set ***A*** is convex. The set ***B*** is not. A set is convex if every line segment with end points in the set is totally subsumed in the set.

A. *CONVEX SETS*

A set, ***A,*** is convex if for every vector $\vec{u}_1 \in \boldsymbol{A}$ and every $\vec{u}_2 \in \boldsymbol{A}$, it follows that $\alpha\vec{u}_1 + (1-\alpha)\vec{u}_2 \in \boldsymbol{A}$ for all $0 \leq \alpha \leq 1$. In other words, the line segment connecting $\vec{u}_1$ and $\vec{u}_2$ is totally subsumed in ***A.*** If any portion of the cord connecting two points lies outside of the set, the set is not convex. This is illustrated in Fig. 1. Examples of geometrical convex sets include balls, boxes, lines, line segments, cones, and planes.

Closed convex sets are those that contain their boundaries. In two dimensions, for example, the set of points

$$A, = \{(x, y) | x^2 + y^2 < 1\}$$

is not closed because the points on the circle $x^2 + y^2 = 1$ are not in the set. The set

$$A = \{(x, y) | x^2 + y^2 \leq 1\}$$

is a closed convex set. ***A*** is referred to as the closure of ***A,.*** Henceforth, all convex sets will be considered closed.

Strictly convex sets are those that do not contain any flat boundaries. A ball is strictly convex whereas a box is not. Neither is a line.'

'Rigorously, a set A is strictly convex if for any distinct $\vec{u}_1, \vec{u}_2 \in$ A, $(\vec{u}_1 + \vec{u}_2)/2$ is an interior point of A. A vector $\vec{u}$ is called an *interior* point of closed set A if $\vec{u} \in$ A and $\vec{u} \notin$ Closure[$E -$ A], where ***E*** is the universal set. In other words, an interior point does not lie on the boundary of a closed convex set.

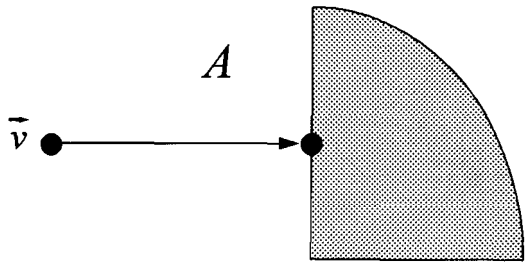

Figure 2 The set A is convex. The projection of $\vec{v}$ onto A is the unique element in A closest to $\vec{v}$.

*B. PROJECTING ONTO A **CONVEX** SET*

The projection onto a convex set is illustrated in Fig. *2*. For a given $\vec{v} \notin$ A, the projection onto A is the unique vector ii $\in$ A such that the distance between ii and $\vec{v}$ is minimum. If $\vec{v} \in$ A, then the projection onto A is $\vec{v}$. In other words, the projection and the vector are the same.

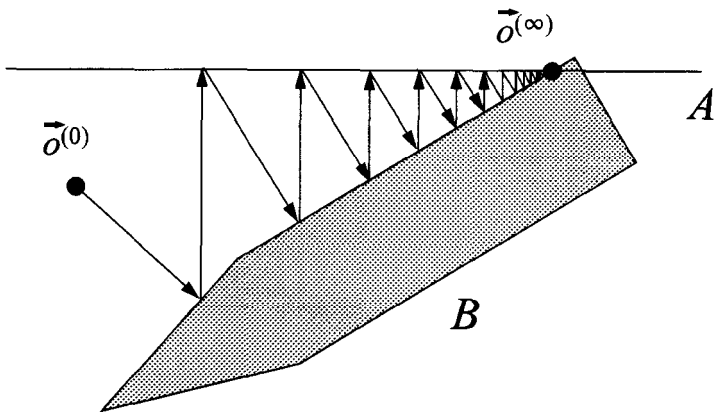

Figure 3 Alternating projection between two or more convex sets with nonempty intersection results in convergence to a fixed point in the intersection. Here, sets A (a Iine segment) and B are convex. Initializing the iteration at $\vec{o}^{(0)}$ results in convergence to $\vec{o}^{(\infty)} \in A \cap B$.

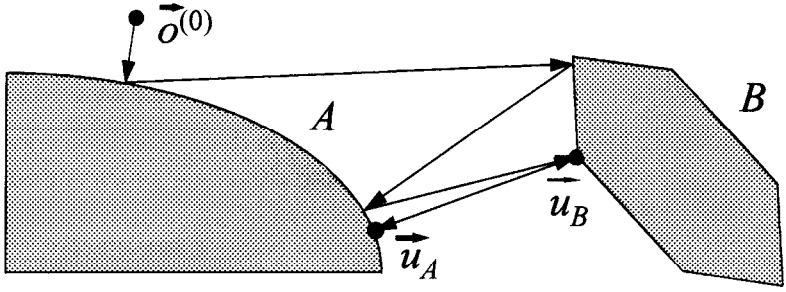

Figure 4 If two convex sets, ***A*** and ***B,*** do not intersect, POCS converges to a limit cycle, here between the points $\vec{u}_A$ and $\vec{u}_B$. The point $\vec{u}_B \in \boldsymbol{B}$ is the point in ***B*** closest to the set ***A*** and $\vec{u}_A \in \boldsymbol{A}$ is the point in ***A*** closest to the set ***B.***

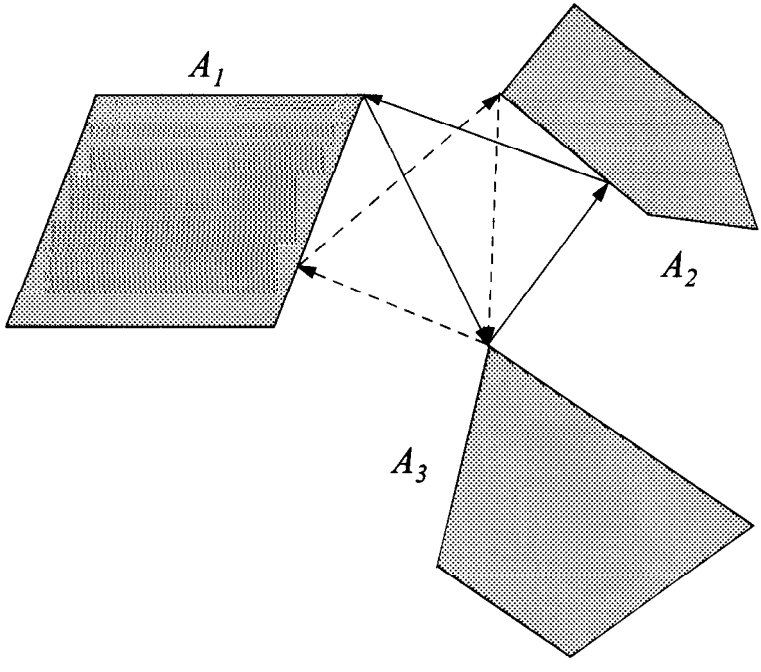

Figure 5 If three or more convex sets do not interest, POCS convergences to greedy limit cycles with no known useful properties; As illustrated here, the limit cycles can differ for different orders of set projection. The limit cycle for the projection order ***A,*** to ***A,*** to ***A,,*** shown by the dashed line, differs from that of ***A,*** to ***A,*** to ***A,.***

C. POCS

There are three outcomes in the application of POCS. Each depends on the various ways that the convex sets intersect.

1. The remarkable primary result of POCS is that, given two or more convex sets with nonempty intersection, alternately projecting among the sets will converge to a point included in the intersection [1, 4]. This is illustrated in Fig. 3. The actual point of convergence will depend on the initialization unless the intersection is a single point.
2. If two convex sets do not intersect, convergence is to a *limit cycle* that is a mean square solution to the problem. Specifically, the cycle is between points in each set that are closest in the mean-square sense to the other set [19]. This is illustrated in Fig. 4.
3. Conventional POCS breaks down in the important case where three or more convex sets do not intersect [21]. POCS converges to *greedy limit cycles* that are dependent on the ordering of the projections and do not display any desirable optimality properties. This is illustrated in Fig. 5.

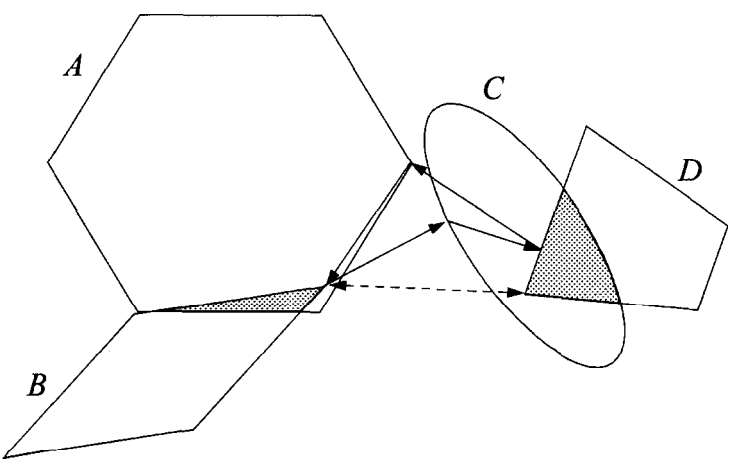

Figure 6 Here, the sets ***A*** and ***B*** intersect as do the sets C and ***D.*** Shown is one of the possible greedy limit cycles resulting from application of POCS. The order of projection is ***A*** to ***B*** to C to ***D.*** The (convex) intersections, $\boldsymbol{A} \cap \boldsymbol{B}$ and $C \cap \boldsymbol{D}$, are shown shaded. Note, though, a greedy limit cycle between the convex sets $\boldsymbol{A} \cap \boldsymbol{B}$ and $C \cap \boldsymbol{D}$ is also possible when using the projection order ***A*** to ***D*** to C to ***B.*** The result is shown by a dashed line. In this case, the limit cycle is akin to that obtained by application of POCS to two nonintersecting convex sets.

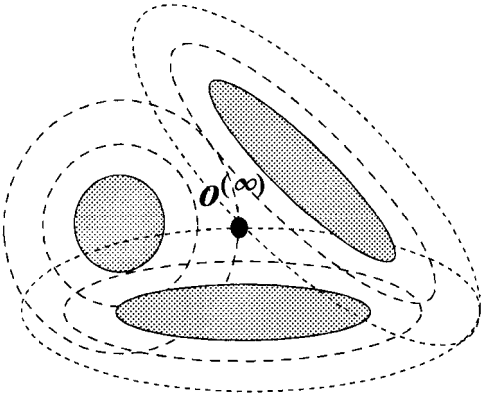

Figure 7 Conventional convex sets can be enlarged (or *fuzzified*) into fuzzy convex sets. Here, the three shaded ellipses correspond to nonintersecting convex sets. Each of the three sets is enlarged to the ellipses shown with the long dashed lines. Enlargement can be done by mathematical morphological dilation of the original convex sets. There is still no intersection among these larger sets, so the sets are enlarged again. Intersection now occurs. The resulting dashed lines are contours, or a-cuts, of fuzzy convex sets. Any group of nonintersecting convex sets can be enlarged sufficiently in this manner so that the enlarged sets (α-cuts) have a finite intersection. Ideally, the minimum enlargement that produces a nonempty intersection is used. A point in that intersection is deemed to be "near" each of the convex sets. In this figure, the point is $o^{(\infty)}$. This point can be obtained by applying conventional POCS to the enlarged sets.

This greedy limit cycle can also occur when some of the convex sets intersect and others do not. This is illustrated in Fig. 6.

Oh and Marks [22] have applied Zadeh's ideas on *fuzzy* convex sets [24] to the case where the convex sets do not intersect. The idea is to find a point that is "near" each of the sets.* Three nonintersecting convex sets are shown in Fig. 7. Each of the convex sets is "enlarged" sufficiently so that the resulting convex sets intersect.† There always exists a degree of

*The term "near" is referred to as a *fuzzy* ***linguistic variable.***

'The enlargement of the set is obtained by ***morphological dilution*** with a convex dilation kernel set. If the kernel is a circle, dilation can be geometrically viewed as the result of rolling the circle on the boundary of the convex set. The larger the diameter of the circle, the greater the dilation. If both A and the dilation kernel set are convex, then so is the dilation. In Fig. 7, enlargement eventually results in the unique intersection point, $o^{(\infty)}$. Description of the details of this process is beyond the scope of this chapter. Details are in the papers by Oh and Marks (22, 23).

enlargement that results in a nonempty intersection of all of the sets.* The smallest enlargement that results in a nonempty intersection is sought. A point in the resulting intersection is then "near" each of the convex sets. Conventional POCS is applied to these sets to find such a point.

III. Convex Sets of Signals

The geometrical view introduced in the previous section allows powerful interpretation of POCS applied in a signal space, $\mathscr{H}$.† For our notation, we will use continuous functions, although the concepts can be easily extended to functions in discrete time."

A. THE SIGNAL SPACE

An image, $u(x)$, is the $\mathscr{H}$ if**

$$\|u(x)\| < \infty,$$

where the norm of $u(x)$ is

$$\|u(x)\| = \sqrt{\int_{-\infty}^{\infty} |u(x)|^2 \, dx}.$$

*Proof: Enlarge each set to fill the whole space.

'More properly, a Hilbert or L_2 space (20).

"That is, from an L_2 to an 1, space. One advantage of discrete time is the guaranteed strong convergence of POCS. Denote the nth element of a sequence u by $u[n]$ and let $o^{(k)}[n]$ be the kth POCS iteration. Let $o[n]$ be the point of convergence and $u[n]$ is any point (including the origin) in l_2, then

$$\lim_{k \to \infty} \|u[n] - o^{(k)}[n]\|^2 = \|u[n] - o[n]\|^2$$

for all $u[n]$. The square of the l_2 norm of a sequence $u[n]$ is

$$\|u[n]\|^2 = \sum_{n=-\infty}^{\infty} |u[n]|^2.$$

In continuous time, only weak convergence can generally be assured [4]. Specifically,

$$\lim_{n \to \infty} \int_{-\infty}^{\infty} u(x) o^{(n)}(x) \, dx = \int_{-\infty}^{\infty} u(x) o(x) \, dx$$

for all $u(x)$ is L_2. Strong convergence assures weak convergence.

**Signals in a Hilbert space are also required to be Lebesgue measurable, although this will not be of concern in our treatment.

The *energy* of $u(x)$ is

$$E = \|u(x)\|^2. \tag{1}$$

The signal space thus consists of all finite energy signals. Geometrically, $\vec{x} = u(x)$ can be visualized as a point in the signal space a distance of $\|u(x)\|$ from the origin, $u(x) \equiv 0$. Similarly, the (mean square) distance between two points $u(x)$ and $v(x)$ is simply $\|u(x) - v(x)\|$.

Two objects, $w(x)$ and $z(x)$, are said to be *orthogonal* if

$$\int_{-\infty}^{\infty} w(x) z^*(x)\, dx = 0, \tag{2}$$

where the superscript asterisk denotes complex conjugation.

Some examples of signal sets follow.

1. Convex Sets

Analogous to the definition given for sets of vectors, a set of signals, A, is convex if, for $0 \leq \alpha \leq 1$, the signal

$$\alpha u_1(x) + (1 - \alpha) u_2(x) \in A \tag{3}$$

when $u_1(x), u_2(x) \in$ A.

2. Subspaces

Subspaces (also called linear manifolds) can be visualized as hyperplanes in the signal space. A set of signals, $\mathscr{S}$, is a subspace if

$$\beta u_1(x) + \gamma u_2(x) \in \mathscr{S} \tag{4}$$

when $u_1(x)$, u,(x) $\in \mathscr{S}$, and β, γ are any finite real numbers. Comparing Eq. (4) with Eq. (3) reveals that, in the same sense that lines and planes are geometrically convex, so are subspaces convex in signal space. The origin, $u(x) \equiv 0$, is an element of all subspaces.[‡]

3. Linear Varieties

A *linear variety* [20] is any hyperplane in the signal space. It need not go through the origin. All subspaces are linear varieties. A linear variety, $\mathscr{L}$, can always be defined as

$$\mathscr{L} = \{\mathrm{U(X)} = u_{\mathscr{S}}(x) + d(x) | u_{\mathscr{S}}(x) \in \mathscr{S}\},$$

[‡] If $u(x) \in \mathscr{S}$, then, with $u_1(x) = u(x) = -u_2(x)$ and $\beta = \gamma = 1$, we have, from Eq. (4), that $0 = u(x) - u(x) \in \mathscr{S}$.

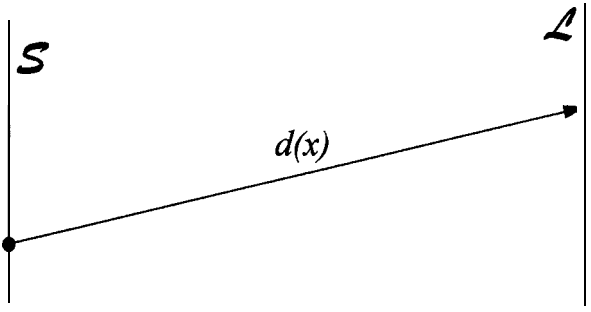

Figure 8 The subspace, $\mathscr{S}$, is shown here as a line. The function d(x), assumed not to lie in the subspace, $\mathscr{S}$, is a displacement vector. The tail of the vector, d(x), is at the origin [u(x) ≡ 0]. The set of all points in $\mathscr{S}$ added to d(x) forms the linear variety, $\mathscr{L}$.

where $\mathscr{S}$ is a subspace and d(x) $\notin \mathscr{S}$ is a displacement vector. The formation of a linear variety from a subspace is illustrated in Fig. 8.

4. Cones

A *cone* with its vertex at the origin is a convex set. If $u(x) \in$ cone, then au(x) $\in$ cone for all $\alpha > 0$. Orthants* and line segments drawn from the origin to infinity in any direction are examples of cones.

B. SOME COMMONLY USED CONVEX SETS OF SIGNALS

A number of commonly used signal classes are convex. In this section, examples of these sets and their projection operators are given. Projection operators will be denoted by a $\mathscr{P}$. The notation

$$u(x) = \mathscr{P}_{\mathrm{K}} v(x)$$

is read "$u(x)$ is the projection of $v(x)$ onto the convex set A_{K}." Note, if $v(x) \in$ A,, then $\mathscr{P}_{\mathrm{K}} v(x) = v(x)$. Also, projection operators are *idempotent* in that

$$\mathscr{P}_{\mathrm{K}}^2 = \mathscr{P}_{\mathrm{K}}.$$

In other words, once one projects onto a convex set, an additional projection onto the same convex set results in no change. Most projections

*In two dimensions, an orthant is a quadrant; in three, an octant.

are intuitively straightforward. In many instances, the projection is obtained simply by forcing the signal to conform with the constraint in the most obvious way.

In the definition of some sets and projections, the Fourier transform of a signal is used. It is defined by

$$U(\omega) = \int_{-\infty}^{\infty} u(x)e^{-j\omega x}\,dx.$$

The inverse Fourier transform is

$$u(x) = \frac{1}{2\pi}\int_{-\infty}^{\infty} U(\omega)e^{j\omega x}\,d\omega.$$

1. Band-Limited Signal

The set of band-limited signals with bandwidth Ω is

$$\boldsymbol{A}_{\mathrm{BL}} = \{u(x)|U(\omega) = 0 \quad \text{for } |\omega| > \Omega\}. \tag{5}$$

The set, A_{BL}, is a subspace because $\beta u_1(x) + \gamma u_2(x)$ is band limited when both $u_1(x)$ and $u_2(x)$ are band limited. To project an arbitrary signal, $v(x)$, onto A_{BL}, the Fourier transform, $V(\omega)$, is first evaluated:

$$\begin{aligned} u(x) &= \mathscr{P}_{\mathrm{BL}} v(x) \\ &= \frac{1}{2\pi}\int_{-\Omega}^{\Omega} V(\omega)e^{j\omega x}\,\boldsymbol{dw}. \end{aligned} \tag{6}$$

In other words, $u(x)$ is obtained by passing $v(x)$ through a low-pass filter.

2. Duration Limited

The convex set of duration-limited signals is, for a given $X > 0$,

$$\boldsymbol{A}_{\mathrm{TL}} = \{u(x)|u(x) = 0 \quad \text{for } |x| > X\}. \tag{7}$$

Because the weighted sum of any two duration-limited signals is duration limited, the set $\boldsymbol{A}_{,,}$ is recognized as a subspace. To project an arbitrary $v(x)$ onto this set, the portion of $v(x)$ for $|x| > \mathrm{X}$ is simply set to zero.

$$\begin{aligned} u(x) &= \mathscr{P}_{\mathrm{TL}} v(x) \\ &= \begin{cases} v(x), & |x| \le \mathrm{X}, \\ 0, & |x| > \mathrm{X}. \end{cases} \end{aligned} \tag{8}$$

3. Real Transform Positivity

The set of signals with real and positive Fourier transform is

$$\boldsymbol{A}_{\mathrm{POS}} = \{u(x) | \mathscr{R}U(\omega) \geq 0\}, \tag{9}$$

with $\mathscr{R}$ denotes "the real part of." The set $\boldsymbol{A}_{,,}$ is a cone. To project onto this set, the Fourier transform of $v(x)$ is first evaluated. The projection follows as

$$\begin{aligned} u(x) &= \mathscr{P}_{\mathrm{POS}} v(x) \\ &= \frac{1}{2\pi} \int_{-\infty}^{\infty} j\mathscr{I}V(\omega)[\mathrm{POS}\, \mathscr{R}V(\omega)] e^{j\omega x}\, \mathrm{do}. \end{aligned} \tag{10}$$

where POS performs a positive value operation and $\mathscr{I}$ denotes the "imaginary part of." In other words, the Fourier transform is made to be real and positive and is then inverse transformed to find the projection onto $\boldsymbol{A}_{,,,}$.

4. Constant Area

Over a given interval, $2a$, the set of signals with given area, ρ, is

$$A_{\mathrm{CA}} = \left\{ u(x) \Big| \int_{-a}^{a} u(x)\, dx = \rho \right\}.$$

This is a linear variety. The subspace that is displaced to form $\boldsymbol{A}_{,,}$ is that corresponding to $\rho = 0$. For $|x| \leq$ a, a displacement vector is d(x) = $\rho/(2a)$.

5. Bounded Energy

The set of signals with bounded energy, for a given bound η, is

$$\boldsymbol{A}_{\mathrm{BE}} = \{u(x) | E \leq \eta\},$$

where $\boldsymbol{E}$ is defined in Eq. (1). The set $\boldsymbol{A}_{,,}$ is a ball. The projection follows as

$$\begin{aligned} u(x) &= \mathscr{P}_{\mathrm{BE}} v(x) \\ &= \begin{cases} v(x), & \|v(x)\|^2 \leq \eta, \\ \dfrac{\sqrt{\eta}\, v(x)}{\|v(x)\|}, & \|v(x)\|^2 > \eta. \end{cases} \end{aligned}$$

6. Constant Phase

The convex set of signals whose Fourier transform has a specific phase, $\varphi(\omega)$, is

$$A_{CP} = \{u(x)|\theta(\omega) = \varphi(\omega)\},$$

where arg $U(\omega) = \theta(\omega)$.*

7. Bounded Signals

For a given real signal, $a(x)$, the set of bounded signals

$$A_{BS} = \{u(x)|\mathscr{R}u(x) \leq a(x)\}$$

is convex. If $a(x) \equiv$ constant, then A_{BS} is a box. As in other cases, the choice of projection is obvious. The signal is set to $\mathscr{R}u(x) = a(x)$ if $\mathscr{R}v(x)$ is too large. Otherwise, the signal remains as is.

$$u(x) = \mathscr{P}_{BS}v(x)$$
$$= \begin{cases} v(x); & \mathscr{R}v(x) \leq a(x) \\ a(x) + j\mathscr{I}v(x); & \mathscr{R}v(x) > a(x). \end{cases}$$

8. Signals With Identical Middles

Let $a(x)$ be a given signal on the interval $|x| \leq$ X. Define

$$A_{IM} = \{u(x)|u(x) = a(x) \quad \text{for } |x| \leq X; \quad \text{anything for } |x| > X\}. \tag{11}$$

This set is a linear variety. The parallel subspace corresponds to $a(x) = 0$ and the displacement vector is d(x) = $a(x)$. To project onto A_{IM}, one merely inserts the desired signal, $a(x)$, into the appropriate interval.

$$u(x) = \mathscr{P}_{IM}v(x)$$
$$= \begin{cases} a(x), & |x| \leq X, \\ v(x), & |x| > X. \end{cases}$$

*In other words, the transform can be written in polar form as $U(\omega) = A(\omega)e^{j\theta(\omega)}$.

IV. Examples

A number of commonly used reconstruction and synthesis algorithms are special cases of POCS. In this section, we look at some specific examples.

A. VON NEUMANN'S ALTERNATING PROJECTION THEOREM

When all of the convex sets are linear varieties, POCS is equivalent to Von Neumann's alternating projection theorem (2.5).

B. THE PAPOULIS-GERCHBERG ALGORITHM

The Papoulis-Gerchberg algorithm is a method to restore band-limited signals when only a portion of the signal is known. It is a special case of POCS.

Given an analytic (entire) function on the complex plane, knowledge of the function within an arbitrarily small interval is sufficient to perform an analytic continuation of the function to the entire complex plane. The value of the function and all of its derivatives can be evaluated at some point interior to the interval and extension performed using a Taylor series. In practice, noise and measurement uncertainty prohibit evaluation of all derivatives. If the measurement of only the first three derivatives can be done with some degree of certainty, for example, only a cubic polynomial could be fitted to the point.

A Taylor series expansion at a point does not use all of the known values of the function within the interval. Slepian and Pollak [26, 271 were the first to explore analytically the possibility of reconstructing a band-limited signal* using all of the known portion of the signal. Using prolate spheroidal wave function analysis, Slepian was able to show that the restoration problem is ill-posed.

Papoulis [28–30] and later Gerchberg [31] formulated a more straightforward, intuitive, and simple technique [27] for the same problem considered by Slepian. Assume we are given a portion of a band-limited object, o(x):

$$i(x) = \begin{cases} o(x), & |x| \le X, \\ 0, & |x| > X. \end{cases}$$

*All bandlimited signals are analytic (entire) everywhere on the finite complex plane.

We further assume we know the bandwidth, Ω, of $o(x)$. The Papoulis-Gerchberg algorithm simply alternatingly imposes the requirements that the signal (a) is band-limited and (b) matches the known portion of the signal. It consists of the following steps.

1. Initiate iteration $N = 0$ and $o^{(N)}(x) = i(x)$.
2. Pass $o^{(N)}(x)$ through a low-pass filter with bandwidth Ω.†
3. Set the result of the filtered signal to zero in the interval $|x| \leq X$.
4. Add the known portion of the signal, $i(x)$, over the interval $|x| \leq X$.
5. The new signal, $o^{(N+1)}(t)$, is no longer band limited. Therefore, set $N = N + 1$ and go to step 2. Repeat the process until desired convergence.

This is illustrated in Fig. 9. The numbers in Fig. 9 correspond to the numbered steps above. In the absence of noise, the Papoulis-Gerchberg algorithm has been shown to converge (32) in the sense that

$$\lim_{N \to \infty} \|o(x) - o^{(N)}(x)\| = 0.$$

Restoration of a band-limited signal knowing only a finite portion of the signal and the signal's bandwidth is ill-posed. In other words, a small bounded perturbation on $i(x)$ cannot guarantee a bounded error on the restoration. However, (1) additional, possibly nonlinear, constraints can be straightforwardly added to the iteration to improve the problem's posedness; (2) numerical results are typically good "near" where the signal is known-the restoration is known to be band limited and therefore smooth; and (3) the problem described is one of *extrapolation*. The Papoulis-Gerchberg algorithm can also be applied to interpolation, i.e., finding $o(x)$ from $o(x) - i(x)$; interpolation is well posed (32).

Youla [33] was the first to recognize the Papoulis-Gerchberg algorithm as a special case of POCS between a subspace and a linear variety. There are two convex sets:

1. The set of all signals equal to $o(x)$ on the interval $|x| \leq X$‡:

$$\boldsymbol{A}_{\mathrm{IM}} = \{u(x) | u(x) = i(x), \quad |x| \leq X\}.$$

†That is, Fourier transform $o^{(N)}(x)$, set the transform equal to zero for $|\omega| > \Omega$ and inverse transform.

‡Equivalent to the definition in Eq. 7 with middle $m(x)$ = i(x).

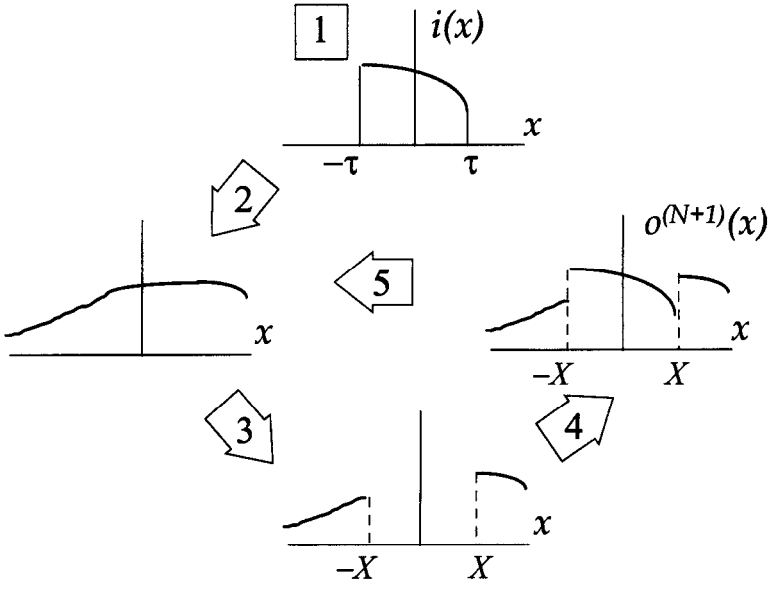

Figure 9 Illustration of the Papoulis-Gerchberg algorithm. Because no signal that is time limited can be band limited, the first estimate, $o^{(N)}(x)$ = i(x) (N = 0), is incorrect. It is made band limited by the process of low-pass filtering. The bandwidth of the filter is Ω. The new signal no longer matches $o(x)$ in the middle. Thus, the signal is set to zero on the interval $|x| \leq$ X and the known portion of the signal is added. The result, $o^{(N+1)}(x)$, is no longer band limited. The sharp discontinuities at the edges prohibit it from being so. Therefore, it is made band limited by the process of low-pass filtering. The process is repeated until the desired accuracy is achieved.

2. The set of all band-limited signals, A_{BL}, with a bandwidth Ω or less. This set is defined in Eq. (5).

The geometry of the Papoulis-Gerchberg algorithm in a signal space is illustrated in Fig. 10. Shown is the subspace, A_{BL}, consisting of all band-limited signals with a bandwidth not exceeding Ω. Also shown is the subspace $A_{,,=0}$ consisting of all signals that are identically zero in the interval $|x| \leq$ X. Consider the set

$$A, = \{u(x) | u(x) = 0, \quad |x| > X\}.$$

The subspace $A_{\perp}$ is orthogonal* to $A_{IM=0}$ because, for every $w(x) \in$

*$A_{\perp}$ is said to be the orthogonal *complement* of $A_{IM=0}$. Note that, if $\mathscr{P}_{IM}$ projects onto $A_{,,=0}$ then $1 - \mathscr{P}_{IM}$ projects onto $A_{\perp}$ where 1 is an identity operator.

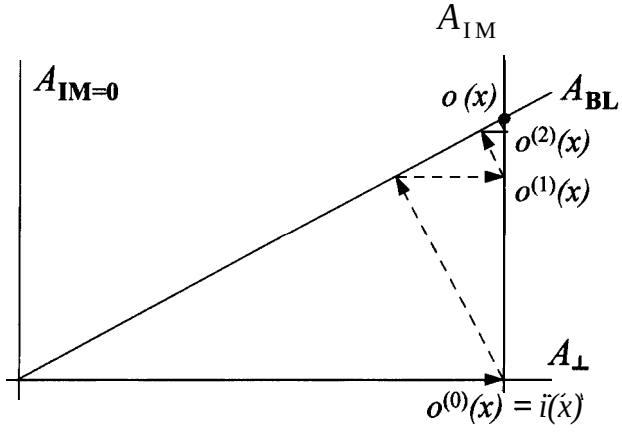

Figure 10 The Papoulis-Gerchberg algorithm in signal space. The two convex sets are (1) a (subspace) set of band-limited signals and (2) the linear variety of all signals with $i(x)$ in the middle.

$A_{IM=0}$ and $z(x) \in A_{\perp}$, Eq. (2) is true.† As always, the origin $[u(x) \equiv 0]$ is common to all of the subspaces.

The known portion of the signal, *i(x),* clearly lies on the subspace, $A_{\perp}$. The signal to be recovered, $o(x)$, lies on the $A_{,,}$ subspace. As illustrated in Fig. 10, the given signal, *i(x),* can be visualized as the projection of $o(x)$ onto the subspace $A_{\perp}$. The linear variety, $A_{,,,}$ in Fig. 10 is the displacement of the subspace, $A_{IM=0}$, by the orthogonal vector, *i(x).*

In the signal space setting of Fig. 10 the Papoulis-Gerchberg algorithm can be described. The signal to be restored, $o(x)$, lies on the intersection of band-limited signals (A_{BL}) and the set of signals equal to *i(x)* in the middle (A_{IM}). We know only that the signal to be reconstructed looks like *i(x)* in the middle and lies somewhere in the space of band-limited signals.

Beginning with the initialization, $o^{(0)}(x) = i(x)$, *we* perform a low-pass filter operation. This is equivalent to projecting *i(x)* onto the subspace of band-limited signals. The next step, as illustrated in Fig. 9, is to throw away the middle of the signal. This is the equivalent in Fig. 10 of projecting onto the $A_{,,=0}$ subspace. To this signal, we vectorally add *i(x)* to obtain $o^{(1)}(x)$. The process is repeated. The signal $o^{(1)}(x)$ is projected onto the set of band-limited signals, projected onto $A_{,,=0}$, and then added to *i(x)* to

†Indeed, $w(x)z^*(x) = 0$.

form $o^{(2)}(x)$, etc. Clearly, the iteration is working its way along the set A,, toward the desired result, $o(x)$.

The alternating projections in the Papoulis-Gerchberg algorithm are performed between the subspace A,, and the linear variety A,,. Inspection of Section IV.A reveals the Papoulis-Gerchberg algorithm as a special case of Von Neumann's alternating projection theorem.

C. HOWARD'S MINIMUM-NEGATMTY-CONSTRAINT ALGORITHM

Howard [34, 35] proposed a procedure for extrapolation of a interferometric signal known in a specified interval when the spectrum of the signal was known (or desired) to be real and nonnegative. The technique was applied to experimental inteferometric data and performs quite well.

As shown by Cheung *et al.* (36), Howard's procedure was a special case of POCS. Iteration is between the cone of signals with non-negative Fourier transforms defined by A,,, in Eq. (9) and the set of signals with identical middles, A,, , as defined in Eq. (11). As with the Papoulis-Gerchberg algorithm, the middle is equal to the known portion of the signal.

The geometrical interpretation of Howard's minimum-negativity-constraint algorithm is similar to that of the Papoulis-Gerchberg algorithm pictured in Fig. 10, except that the subspace A,, is replaced by a cone corresponding to A,,,.

D. RESTORATION OF LINEAR DEGRADATION

In this section, POCS is applied to a linear degradation of a discrete time signal. Denote the degradation operator by the matrix S and the degradation by

$$\vec{i} = \text{so}'. \tag{12}$$

If the degradation matrix, **S**, is not full rank, a popular estimate of $\vec{o}$ is the *pseudo-inverse* *

$$\vec{o}_{\text{PI}} = [\mathbf{S}^T\mathbf{S}]^{-1}\mathbf{S}^T\vec{i}.$$

The *projection matrix*,† $\mathbf{P_S}$, projects onto the column space of S.

$$\mathbf{P_S} = \mathbf{S}[\mathbf{S}^T\mathbf{S}]^{-1}\mathbf{S}^T \tag{13}$$

*The solution, $\vec{o}_{\text{PI}}$, is also referred to as the minimum *norm* solution.

†As is necessary for a projection operator, the projection matrix is idempotent: $\mathbf{P_S^2} = \mathbf{P_S}$.

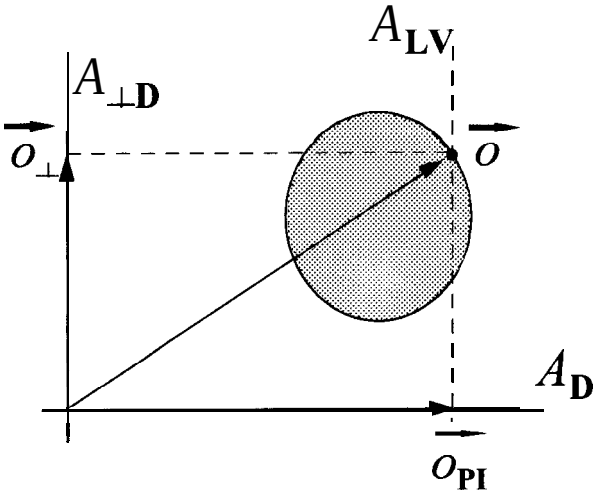

Figure 11 Illustration of restoration of a linear degradation. The signal to be reconstructed, $\vec{o}$, lies both on the linear variety $A_{\perp \mathbf{S}}$ and on the convex set $A_{,}$.

Consider the signal space illustrated in Fig. 11. The pseudo-inverse solution of Eq. (12) lies on the subspace A, onto which $\mathbf{P}_{\mathbf{S}}$ projects. Denote the orthogonal complement of A, by $A_{\perp \mathbf{S}}$. The projection operator onto this space is simply

$$\mathbf{P}_{\mathrm{I}\,\mathrm{S}} = \mathbf{1} - \mathbf{P}_{\mathbf{S}},$$

where **1** is an identity matrix. If the projection onto the orthogonal complement is

$$\vec{o}_{\perp} = \mathbf{P}_{\perp \mathbf{S}} \vec{o},$$

we are assured that

$$\vec{o} = \vec{o}_{\mathrm{PI}} + \vec{o}_{\perp} . \tag{14}$$

Define the linear variety

$$\boldsymbol{A}_{\mathrm{LV}} = \left\{ \vec{u} \mid \vec{u} = \vec{\imath} + \mathbf{P}_{\perp \mathbf{S}} \vec{v} \right\},$$

where $\vec{v}$ is any vector in the space.

The pseudo-inverse solution can be improved using POCS if $\vec{o}$ is also known to satisfy one or more convex constraints. In other words

$$\vec{o} \in A_m,$$

where $\{A_m | 1 \le m \le M\}$ is the set of constraint sets and M is the number of constraints. A set of corresponding projection operators can be defined:

$$\{\mathscr{P}_m | 1 \le m \le M\}. \tag{15}$$

In other words, $\mathscr{P}_m$ projects an arbitrary signal onto A,.* Because the desired solution, $\vec{o}$, is known to lie in each of the constraint sets, it follows that

$$\mathscr{P}_m \vec{o} = \vec{o}, \qquad 1 \le m \le M, \tag{16}$$

and

$$\begin{aligned} \vec{o} &= \mathscr{P}_M \mathscr{P}_{M-1} \cdots \mathscr{P}_2 \mathscr{P}_1 \vec{o} \\ &= \mathscr{P}_{\mathscr{C}} \vec{o}, \end{aligned} \tag{17}$$

where

$$\mathscr{P}_{\mathscr{C}} = \mathscr{P}_M \mathscr{P}_{M-1} \cdots \mathscr{P}_2 \mathscr{P}_1. \tag{18}$$

Correspondingly, define the (nonempty) convex set

$$A_{\mathscr{C}} = \mathrm{A}, \cap A_{M-1} \cap \cdots \cap A_2 \cap A_1,$$

where $\cap$ denotes intersection. Note that $\mathscr{P}_{\mathscr{C}}$ does not project onto A,. As illustrated in Fig. 11, the desired signal to be reconstructed, $\vec{o}$, is known to lie both in the convex set A, and the set A,,. A point in the intersection of these sets can be found using POCS. We have the POCS iteration

$$\begin{aligned} \vec{o}_{(N+1)} &= \mathscr{P}_{\mathrm{LV}} \mathscr{P}_M \mathscr{P}_{M-1} \cdots \mathscr{P}_2 \mathscr{P}_1 \vec{o}_{(N)} \\ &= \mathscr{P}_{\mathrm{LV}} \mathscr{P}_{\mathscr{C}} \vec{o}_{(N)} \\ &= \vec{t} + (\mathbf{I} - \mathbf{P_S}) \mathscr{P}_{\mathscr{C}} \vec{o}_{(N)} \end{aligned} \tag{19}$$

The iteration is guaranteed to converge to a point on a solution set,

$$A_{\mathrm{solution}} = A_{\mathscr{C}} \cap A_{\mathrm{LV}}.$$

The solution will, in general, be nearer to $\vec{o}$ in the mean-square sense than was the pseudo-inverse. If A_{solution} consists of a single point, the solution will be unique.

The restoration in Eq. (19) is a generalization of (1) the Papoulis-Gerchberg algorithm for $\mathscr{P}_{\mathscr{C}} = \mathscr{P}_{\mathrm{BL}}$ in Eq. (6) and (2) Howard's algorithm for $\mathscr{P}_{\mathscr{C}} = \mathscr{P}_{\mathrm{POS}}$ in Eq. (10).

*When A, is a subspace, the projection operator is a matrix. That is, $\mathscr{P}_m = \mathbf{P}_m$.

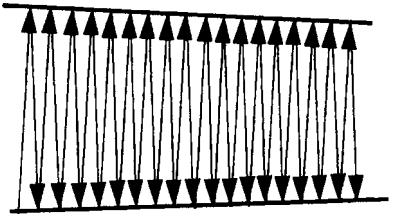

Figure 12 A geometrical example of slowly converging POCS. The intersection of the two linear varieties, far to the right, is the ultimate fixed point of the iteration.

V. Notes

In certain instances, POCS can converge painfully slowly. An example is shown in Fig. 12. One technique to accelerate convergence is relaxing the projection operation by using a relaxed projection with parameter λ [4]:

$$\mathscr{P}_{\text{relaxed}} = \lambda\mathscr{P} + (I - \lambda)I. \tag{20}$$

An operator, $\mathscr{O}$, is said to be *contractive* if, for all $\vec{w}$ and $\vec{z}$,

$$\|\mathscr{O}\vec{w} - \mathscr{O}\vec{z}\| < \|\vec{w} - \vec{z}\|. \tag{21}$$

In other words, operating on the two vectors places them closer together. This is illustrated in Fig. 13. A useful property of contractive operators (37) is, for any initialization, the iteration

$$\vec{o}^{(N+1)} = \mathscr{O}\vec{o}^{(N)} \tag{22}$$

converges to a unique fixed point

$$\vec{o}^{(\infty)} = \mathscr{O}\vec{o}^{(\infty)}.$$

A POCS projection is, however, not contractive.† Projection operators, though, are ***nonexpansive.*** The $\mathscr{O}$ operator is nonexpansive if

$$\|\mathscr{O}\vec{w} - \mathscr{O}\vec{z}\| \leq \|\vec{w} - \vec{z}\|.$$

For nonexpansive operators, the iteration in Eq. (22) can converge to a number of fixed points. A relaxed nonexpansive operator, as in Eq. (20),

†If, for example, both $\vec{w}$ and $\vec{z}$ are in the convex set, and $\mathscr{O}$ is a projection operator, then $\|\mathscr{O}\vec{w} - \mathscr{O}\vec{z}\| = \|\vec{w} - \vec{z}\|$ and Eq. (21) is violated.

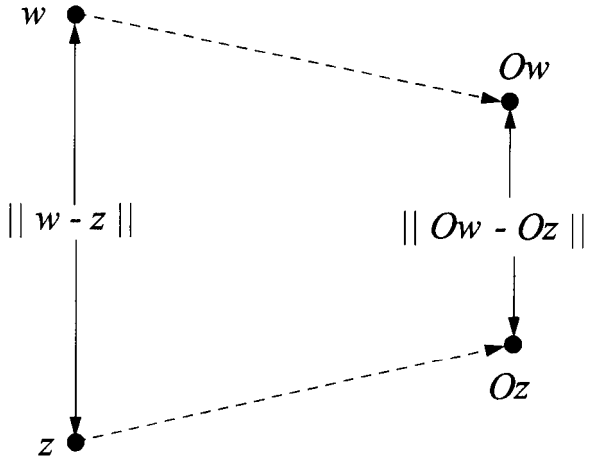

Figure 13 A geometrical example of slowly converging POCS. The intersection of the two linear varieties, far to the right, is the ultimate fixed point of the iteration.

however, is contractive (19). Applications of contractive operators do not have the elegant geometrical interpretation of POCS.

VI. Conclusions

Restoration of degraded signals can, in many cases, be posed as a special case of alternating projection onto convex sets, or POCS. The object to be restored is known to lie in two or more convex constraint sets. Restoration can be achieved by projecting alternately on each of the sets. If the sets have a nonempty intersection, then the projection will approach a fixed point lying in the intersection of the sets. If there are two sets that do not intersect, POCS will converge to a minimum mean-square error solution. If there are three or more sets with empty intersection, POCS yields results that are not generally useful. Fuzzy POCS, however, can be used to obtain a result that is "close" to each of the constraint sets.

POCS is particularly useful in ill-posed deconvolution problems. The problem is regularized by imposing possibly nonlinear convex constraints on the solution set. Using the projection onto to the column space of the convolution kernel as one of the constraints, POCS can be used, in many cases, to craft a desired result.

References

1. H. Stark, editor, "Image Recovery: Theory and Application." Academic Press, Orlando, Florida, 1987.
2. L. M. Bregman, Finding the common point of convex sets by the method of successive projections. *Dokl. Akud. Nauk. SSSR, 162 (No. 3), 487-490 (1965).*
3. L. G. Gubin, B. T. Polyak, and E. V. Raik, The method of projections for finding the common point if convex sets. *USSR Comput. Math. Math.* Phys. (*Engl. Transl.*) 7 (No. 6), l-24 (1967).
4. D. C. Youla and H. Webb, Image restoration by method of convex set projections: Part I-Theory. *IEEE Transactions on Medical Imaging* **MI-l, 81-94 (1982).**
5. M. I. Sezan and H. Stark, Image restoration by method of convex set projections: Part II-Applications and Numerical Results. *IEEE Transactions on Medical Imaging* **MI-l,** 95−101 **(1982).**
6. **S. J. Yen and** H. Stark, Iterative and one-step reconstruction from nonuniform samples by convex projections. *J. Opt. Soc. Am. A 7, 491-499 (1990).*
7. Hui Peng and H. Stark, Signal recovery with similarity constraints. *J. Opt. Soc.* Am. *A* 6 (No. 6), 844-851 (1989).
8. R. J. Marks II and D. K. Smith, Gerchberg-type linear deconvolution and extrapolation algorithms. In "Transformations in Optical Signal Processing" (W. T. Rhodes, J. R. Fienup, and B. E. A. Saleh, eds.), SPIE 373, pp. 161-178 (1984).
9. M. Ibrahim Sezan, H. Stark, and Shu-Jen Yeh, Projection method formulations of Hopfield-type associative memory neural networks. *Appl. Opt. 29 (No. 17) 2616-2622 (1990).*
10. Shu-jeh Yeh and H. Stark, Learning in neural nets using projection methods. *Optical Computing and Processing* **1 (No.** 1), 47-59 (1991).
11. R. J. Marks II, A class of continuous level associative memory neural nets. *Appl. Opt. 26, 2005-2009 (1987).*
12. R. J. Marks II, S. Oh, and L. E. Atlas, Alternating projection neural networks. *IEEE Trans. Circuits Syst. 36, 846-857 (1989).*
13. S. Oh, R. J. Marks II, and D. Sarr, Homogeneous alternating projection neural networks. *Neurocomputing 3, 69-95* (1991).
14. R. J. Marks II, (ed.) "Advanced Topics in Shannon Sampling and Interpolation Theory." Springer-Verlag, Berlin, 1993.
15. S. Oh, C. Ramon, M. G. Meyer, and R. J. Marks II, Resolution enhancement of biomagnetic images using the method of alternating projections. *IEEE Trans. Biomed. Eng. 40 (No. 4), 323-328 (1993).*
16. S. Oh, R. J. Marks II, L. E. Atlas, and J. W. Pitton, Kernel synthesis for generalized time-frequency distributions using the method of projection onto convex sets. *SPIE Proc. Znt. Soc. Opt.* Eng. 1348, 197-207, (1990).

17. S. Oh, R. J. Marks II, and L. E. Atlas, Kernel synthesis for generalized time-frequency distributions using the method of alternating projections onto convex sets. *IEEE* Transactions on *Signal Processing* 42 (No. 7), 1653-1661 (1994).
18. P. L. Combettes, The Foundation of Set Theoretic Estimation. *Proc. IEEE* 81, 182-208 (19931.
19. M. H. Goldburg and R. J. Marks II, Signal synthesis in the presence of an inconsistent set of constraints. *IEEE Trans. Circuits Syst. CAS-32 647-663 (1985).*
20. D. G. Luenberger, "Optimization by Vector Space Methods." Wiley, New York, 1969.
21. D. C. Youla and V. Velasco, Extensions of a result on the synthesis of signals in the presence of inconsistent constraints. *IEEE Trans. Circuits Syst. CAS-33 (No.* 4), *465-468 (1986).*
22. *S.* Oh and R. J. Marks II, Alternating projections onto fuzzy convex sets. *Proceedings of the Second IEEE International Conference on Fuzzy Systems, (FUZZ-IEEE '93), San Francisco, March 1993* 1, 148-155 (1993).
23. R. J. Marks II, L. Laybourn, S. Lee, and S. Oh, Fuzzy and extra-crisp alternating projection onto convex sets (POCS). *Proceedings of the International Conference on Fuzzy Systems (FUZZ-IEEE),* Yokohama, Japan, March, 20-24, 1995, pp. 427-435 (1995).
24. L. A. Zadeh, Fuzzy sets. *Information and Control 8, 338-353 (1965);* reprinted in J. C. Bezdek, (ed.) "Fuzzy Models for Pattern Recognition" IEEE Press, 1992.
25. J. Von Neumann, "The Geometry of Orthogonal Spaces." Princeton Univ. Press, Princeton, New Jersey, 1950.
26. D. Slepian and H. 0. Pollak. Prolate spheroidal wave function Fourier analysis and uncertainty I. *Bell Syst.* Tech. *J.* 40, 43-63 (1961).
27. R. J. Marks II, "Introduction to Shannon Sampling and Interpolation Theory." Springer-Verlag, Berlin, 1991.
28. A. Papoulis, A new method of image restoration. *Joint Services Technical Activity Report 39 (1973-1974).*
29. A. Papoulis, A new algorithm in spectral analysis and bandlimited signal extrapolation. *IEEE Trans. Circuits Syst. CAS-22, 735-742 (1975).*
30. A. Papoulis, "Signal Analysis." McGraw-Hill, New York, 1977.
31. R. W. Gerchberg, Super-resolution through error energy reduction. *Opt. Acta 21, 709-720 (1974).*
32. R. J. Marks II. "Introduction to Shannon Sampling and Interpolation Theory." Springer-Verlag, Berlin, 1991.
33. D. C. Youla, Generalized image restoration by method of alternating orthogonal projections. *IEEE Trans. Circuits Syst. CAS-25, 694-702 (1978).*

34. S. J. Howard, Fast algorithm for implementing the minimum-negativity constraint for Fourier spectrum extrapolation. *Appl. Opt.* 25, 1670-1675 (1986).
35. S. J. Howard, Continuation of discrete Fourier spectra using minimum-negativity constraint. *J. Opt. Soc. Am.* **71, 819-824 (1981).**
36. K. F. Cheung, R. J. Marks II, and L. E. Atlas, Convergence of Howard's minimum negativity constraint extrapolation algorithm. *J. Opt. Soc. Am. A* **5,** 2008-2009 (1988).
37. A. W. Naylor and G. R. Sell, "Linear Operator Theory in Engineering and Science." Springer-Verlag, New York, 1982.

Deconvolution of Images and Spectra

Second Edition

Edited by

Peter A. Jansson

E. I. DU PONT DE NEMOURS AND COMPANY (INC.)
EXPERIMENTAL STATION
WILMINGTON, DELAWARE

ACADEMIC PRESS

San Diego London Boston
New York Sydney Tokyo Toronto